

Suppressing/enhancing effect of rhenium on helium clusters evolution in tungsten: Dependence on rhenium distribution

Fang-Ya Yue^{a,b}, Yu-Hao Li^{a,b}, Qing-Yuan Ren^{a,b}, Fang-Fei Ma^{a,b}, Zhong-Zhu Li^{a,b}, Hong-Bo Zhou^{a,b,*}, Huiqiu Deng^c, Ying Zhang^{a,b}, Guang-Hong Lu^{a,b}

^a Department of Physics, Beihang University, Beijing 100191, China

^b Beijing Key Laboratory of Advanced Nuclear Materials and Physics, Beihang University, Beijing 100191, China

^c Department of Applied Physics, School of Physics and Electronics, Hunan University, Changsha 410082, China

ARTICLE INFO

Article history:

Received 18 June 2020

Revised 18 September 2020

Accepted 20 September 2020

Available online 25 September 2020

Keywords:

Helium clusters

Rhenium

Tungsten

Distribution

Suppressing/enhancing effect

ABSTRACT

The influence of rhenium (Re) on helium (He) evolution in tungsten (W) with different Re distribution is investigated using the first-principles calculations in combination with thermodynamic models. It is found that the He behaviors in W-Re system are closely related to the Re distribution. For the dispersed distribution of Re in W, it is found that a single Re atom only has slight effect on the behaviors of a He atom due to the weak interaction of Re-He₁. Interestingly, with the increasing of He numbers, the binding energy between a single Re and He clusters increases rapidly from 0.03 eV for Re-He₁ to 0.72 eV for Re-He₄. Such high binding energy indicates the strong attraction of Re with He clusters in W. This can be rationalized by the large lattice distortion induced by He clusters, which reduces the electron density of He-occupied position and leads to the transition of neighboring Re/W atom from a substitutional site to an interstitial site. Because of the strong attraction of Re with He clusters, the Re addition effectively reduce the mobility of He clusters in W. As for the aggregated Re distribution, the He trapping capability of vacancy is weakened by Re clusters. These results are well consistent with the experimental observed suppressing effects of Re on the He-induced morphology in W. Further, based on the He behaviors in W-Re σ phase, we suppose that He will segregate from bulk W to Re-rich precipitates, thus enhancing the formation of He clusters. Consequently, our calculations suggest that the distribution of Re plays a key role on the He behaviors in W, which provides a good reference for the design and development of W-based alloys.

© 2020 Elsevier B.V. All rights reserved.

1. Introduction

Tungsten (W) and W alloys are regarded as the most potential plasma facing materials (PFMs) in the future magnetic confinement nuclear fusion power reactor, because of their good thermal property, low tritium retention and high sputtering threshold [1–3]. However, W-PFMs will be exposed to severe irradiation, including both plasma (helium/hydrogen isotopes), fusion neutrons and heat fluxes. Such extreme operational environments severely degrade the performance of materials, and thus results in the great concerns for the safety of fusion reactor [4,5]. It is found that the irradiation of high fluxes and low energy He ions dramatically changes the surface morphology of W, leading to the formation of nanobubbles, voids and fuzz [6–11]. These morphologies have deleterious effects on the thermal conductivity and mechanical property

of materials [12–16], and therefore, great efforts have been made to explore the behaviors of He in W [17–19].

Generally, alloying is considered as an effective method to improve the properties of metals [20–22]. Also, it is found that the alloying elements profoundly affect the behaviors of He in W. For example, the blistering and damage depth in W after high energy (22 keV) and high fluxes ($7 \times 10^{20} \text{ m}^{-2} \text{ s}^{-1}$) He irradiation are remarkably mitigated by 5 wt.% vanadium addition, implying that the presence of vanadium suppresses the He-induced irradiation damage [23]. Rhenium (Re), as a very interesting element in W, has a dual characteristic. On the one hand, as a typical alloying element, the Re addition can improve the mechanical property of W, known as “Re ductilizing effect” [24,25]. On the other hand, as the main transmutation production, Re aggravates the irradiation hardening of W due to the clustering of Re atoms, leading to the negative effects on the application of W [26–28]. Nevertheless, either intentionally added or naturally produced during fusion neutron irradiation, the addition of Re will inevitably interact with He in W, and thus affecting the responses of W from He irradiation.

* Corresponding author.

E-mail address: hbzhou@buaa.edu.cn (H.-B. Zhou).

Hence, it is of great importance to determine the Re effects on the He behaviors in W.

It is reported that the Re addition can profoundly affect the He-induced surface modification in W [9,29,30]. For example, Baldwin and Doerner [9] studied the responses of pure W and W-Re alloy to fuzz formation after exposure to He plasma at 900–1320 K with ions energy of 25–60 eV in PISCES-B. In comparison with the thickness of fuzz layer in pure W, that in W-5 wt.%Re and W-10 wt.%Re alloys is reduced 34% and 44% respectively, suggesting the inhibiting effects of Re on the fuzz growth. Similar suppressing effect of Re on the He-induced fuzz formation in W is also observed after He plasma irradiation at high temperature (~1200–1700 K) in the Magnum and Pilot-PSI devices [29]. Recently, by using the transmission electron microscopy and in-situ high-energy (~10 keV) He⁺ ions irradiation at 773–1473 K, the He-induced damage evolution in pure W and W-5 wt.%Re alloy have been investigated [30]. It is observed that the density of He bubbles in W-Re alloy is comparable with that in pure W, while the average size of bubbles in W-Re alloy is slightly (~10–40%) higher. More importantly, the Re addition induces a pronounced change in bubble morphology, from spherical bubbles in pure W to faceted bubbles in W-Re alloy. This is rationalized by the lower internal pressure of bubbles, i.e. a lower He/vacancy ratio for bubbles in W-Re alloy. As demonstrated in above experimental studies, the addition of Re in W will dramatically affect the surface morphology of W after He irradiation, while its physical origin is still unclear.

In order to understand the influence of Re on the He behaviors, many studies have been conducted on the behaviors of He and Re in W as well as their interactions. An interstitial He atom prefers to occupy tetrahedral interstitial site (TIS), while a Re atom is favorable sitting at substitutional site in W [31,32]. There are strong attractive interactions of Re and He with point defects (both vacancy and self-interstitial atoms) in W, indicating the formation of Re-He-vacancy/SIA complexes [33]. Further, the interaction of a substitutional Re atom and an interstitial He atom in W is very weak with the binding energy of ~0.02 eV [34]. Such extremely weak interaction implies the negligible influence of Re on He in W, which is different from the experimental observations. Although above studies provide some references to understand the He behaviors in W-Re system, the underlying mechanism for the influence of Re on the evolution of He as well as its dependence on the Re distribution remain to be elucidated.

In the present study, the effect of Re on He behaviors in W with different Re distribution is investigated using the first-principles method. Interestingly, the binding energy between Re and He clusters increases rapidly with the increasing of He atoms, from 0.03 eV for Re-He₁ to 0.72 eV for Re-He₄. Such high binding energy indicates the strong attraction of Re with He clusters, and thus plays a pinning effect on the migration of He clusters in W. Also, the aggregation of Re atoms increases the He trapping energy in vacancy, leading to the reduction of He/vacancy ratio. These findings give the plausible interpretations for the experimental observation. Further, the dissolution and clustering of He in W-Re σ phase are also determined, and we propose that He atoms will segregate from bulk W to Re-rich phase, enhancing the formation of He clusters. These results will deepen our understanding of the effect of alloying element on the He behaviors in W-PFMs.

2. Computational method

Our density functional theory (DFT) calculations were performed within the Vienna Ab-initio Simulation Package (VASP, v.5.4.1) code with the plane-wave pseudo-potential method [35,36]. The generalized gradient approximation (GGA) developed by Perdew, Burke and Ernzerhof (PBE) was used to describe the exchange and correlation interactions [37]. The correspond-

ing pseudo-potential date-marks are 08Apr2002, 17Jan2003 and 05Jan2001 for W, Re and He, respectively. Through the convergence tests, the cut-off energy was set to be 350 eV and the negligible influence on the results was found with increased cut-off energy. Unless otherwise stated, both the shape and the volume of the supercell as well as the atomic position were fully relaxed. The structural optimization was continued until the forces on all atoms in the supercell less than 0.001 eV/Å. In order to determine the influence of supercell relaxation on the diffusion of He in W/W-Re system, the He diffusion energy barriers were estimated using the conventional climbing image nudged elastic band (CI-NEB) (ISIF = 2 and IOPT = 1) and Solid State CI-NEB (ISIF = 3 and IOPT = 3) method [38]. It is found that the supercell relaxation only has a slight effect on the migration energy barriers of He (<0.004 eV). Therefore, in present work, the migration of He was investigated using the conventional CI-NEB (ISIF = 2 and IOPT = 1) method.

For the body-centered cubic (bcc) system, we have examined our results using different supercell sizes and k-point mesh density. It is found that the results are reasonably converged at 128-atom supercell ($4a_0 \times 4a_0 \times 4a_0$) and $3 \times 3 \times 3$ k-points grid density, which were used in our calculations. The lattice constant of bcc W obtained in our calculation is 3.17 Å, which is consistent with experimental results (3.16 Å in [39,40]). As for the W-Re σ phase, its space group is $P4_2/mnm$ and has five non-equivalent sites. The occupation numbers of these non-equivalent sites are 2, 4, 8, 8 and 8, respectively, and thus the σ phase contains 30 lattice points for the unit cell. Here, we have checked the finite-size effect by calculating the energetic results in W-Re σ phase using 60-atom supercell ($1a_1 \times 1a_2 \times 2a_3$) and 120-atom ($1a_1 \times 1a_2 \times 4a_3$) supercell. It is found that the energetic results of He clusters in W-Re σ phase reasonably converge at the 60-atom supercell in comparison with the 120-atom one. Therefore, the 60-atom supercell is large enough to describe the behaviors of He in W-Re σ phase, and thus was employed in our calculations. The corresponding k-points grid density was $5 \times 5 \times 5$. The calculated lattice parameter for the stable W-Re σ phase is 9.70 Å for a/b and 5.03 Å for c , in a good agreement with the experimental data ($a = 9.627$ Å, $c = 5.015$ Å in [41]). More details for the configuration of W-Re σ phase were presented in our previous study [42].

3. Results and discussions

3.1. Behaviors of He in W-Re system with dispersed Re distribution

3.1.1. Interaction between a single Re and a He atom in W

In order to examine the interaction of Re with He in W, one Re atom is set at a substitutional site in bcc W, and an interstitial He occupies a series of TISs with different distances from Re. The solution energy of He can be expressed as

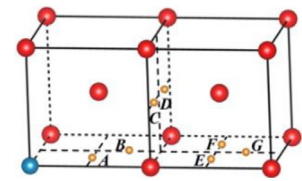
$$E_{\text{He}}^{\text{sol}} = E_{\text{W+Re+He}} - E_{\text{W+Re}} - E_{\text{He}}^{\text{ref}}, \quad (1)$$

where $E_{\text{W+Re+He}}$ and $E_{\text{W+Re}}$ are the energy of 127W-1Re system with and without an interstitial He atom. As for the third term ($E_{\text{He}}^{\text{ref}}$), it is the reference energy of He, which is selected to be the energy of a single He atom in vacuum.

Table 1 shows the He solution energies as a function of different Re-He distances in W-Re system. Here, the results with zero-point energy (ZPE) correction were also provided, because it can play an important role on the behaviors of light elements. It is found that the ZPE correction slightly increases (~0.08 eV) the solution energy of He, while the relative stability of He is unchanged. This is consistent with previous DFT studies [43,44]. Hence, the ZPE corrections are neglected in the following part. As seen in Table 1, the addition of Re only has slight effect on the dissolution of He in W. When a He atom is located at the site A (~2.14 Å

Table 1

The solution energy (E_{sol} and E_{sol}^{ZPE} , eV), electronic contribution (EC , eV), mechanical contribution (MC , eV), volume variation (ΔV , Å³) and electron density (ρ_e^{He} , e/Å³) of an interstitial He atom at various TISs (A-G) in W-Re system. For Reference, the atomic distances (Å) of Re-He pair before and after relaxation are also presented. The red, blue and yellow balls represent W, Re and He atoms, respectively.



		E_{sol}	MC	EC	E_{sol}^{ZPE}	ΔV	ρ_e^{He}	Re-He distance	
								Initial	Final
W-Re	A	6.28	1.35	4.92	6.36	5.67	0.162	1.77	2.14
	B	6.32	1.11	5.21	6.40	5.34	0.174	2.86	2.82
	C	6.32	1.08	5.24	6.40	5.21	0.175	3.63	3.66
	D	6.32	1.09	5.23	6.40	5.38	0.175	4.27	4.27
	E	6.31	1.08	5.23	6.38	5.32	0.174	4.82	4.83
	F	6.31	1.07	5.24	6.39	5.57	0.175	5.32	5.33
	G	6.31	1.07	5.24	6.39	5.55	0.175	5.77	5.77
bcc-W	TIS	6.31	1.07	5.24	6.39	5.54	0.176	/	/

Re-He distance), the corresponding He solution energy is 6.28 eV and slightly lower than that at TIS in bulk W (~6.31 eV). The solution energy reduction indicates the attractive interaction between Re and He in W. Nevertheless, from 2.82 Å to 4.27 Å (site B, C and D), the solution energy of He increases, and becomes 0.01 eV higher than that in W without Re. Beyond 4.27 Å, the He solution energy is independent on the Re-He distance and equals to that in perfect W. Hence, the interaction of a single Re atom with an interstitial He atom in bulk W is extremely weak (~0.03 eV), although there is an attraction of Re-He at first nearest neighboring (1NN) distance.

As well as known, He is a typical noble gas element, and thus it does not tend to interact with other atoms. However, why is there a weak attraction of Re-He in bcc W? To unravel this unexpected attraction, we explore the underlying physics for Re-He interaction by analyzing the solution energies and electronic states. Here, the He solution energy is divided into the electronic contribution (EC) and the mechanical contribution (MC). The EC is the electronic interaction between He and surrounding atoms, which is obtained from the energy difference of solution energy and MC . As for the MC , it represents the deformation energy induced by the embedded He atom that calculated from the energy difference of the systems with and without He atom. As seen in Table 1, the MC is much lower than the EC in all cases, indicating that the poor solubility of He is mainly controlled by the electronic interaction. Further, the EC of He in bulk W is 0.32 eV higher than at site A in W-Re system, leading to the positive effect on the attraction of Re-He, while the corresponding MC difference is -0.28 eV, resulting in the negative effect on the attraction of Re-He. This suggests that the weak attractive interaction of Re-He in W can be attributed to the EC .

As shown in our previous studies [45,46], the EC of He in metals is dependent on the environmental electron density. Since He has a closed shell electronic structure, there is repulsive interaction between He and any electronic environment. This indicates that the He atom is energetically favorable to occupy the positions with low electron density, i.e. the higher the electron density, the higher solution energy of He. As presented in Table 1, the electron density of He at site A in W-Re system is 0.162 e/Å³, lower than that at TIS in bulk W without Re or at other interstitial sites in W-Re system. Here, the electron density is only a value at He-occupied position. In order to obtain this value, a He atom is firstly set at a given location (interstitial site or vacancy center), and both the shape/volume of the supercell and atomic positions are fully relaxed by energy minimization. After that, the He atom is removed, and the atomic coordinates are fixed to perform the

static self-consistent calculations. Accordingly, the electron density of He-occupied position can be obtained. Interestingly, the reduction of electron density at site A is not due to the direct interaction of Re-He, but because of the deformation induced by He addition. Generally, the dissolution of He in W and W-Re system will induce the lattice expansion owing to the small available volume of interstitial sites. Since the Re-W bond in W-Re system is weaker than the W-W bond in bulk W [47], the He-induced expansion in bulk W is smaller than that at site A in W-Re system. This is consistent with the results of ΔV and MC (see Table 1), in which the ΔV and MC of He at site A is higher than other cases. Therefore, the weak attraction of Re-He is attributed to the weakening effect of Re on atomic bond, which promotes the volume expansion induced by He and reduces the electron density nearby, and thus facilitating the dissolution of He in W.

Based on above results, it can be found that the weak attraction of Re with He in W is originated from the lattice distortion induced by He dissolution rather than their direct interaction. Here, to further reproduce the direct interaction of Re-He pair in bcc W, we examine the He solution energies in bulk W and W-Re system (site A) as well as their energy difference under hydrostatic strain. The hydrostatic strain has been imposed in the supercell, and the corresponding lattice constants (a) in the strained systems are expressed as $a = (1 + \varepsilon)a_0$, where ε and a_0 is the given strain value and the lattice constant of the supercell without strain, respectively. In these calculations, the atomic positions are fully fixed in order to avoid the influence of lattice deformation. As presented in Fig. 1, the solution energies of He in bulk W and W-Re system are always positive, which decrease with the increasing of hydrostatic strain (or Re/W-He distance). This indicates that there is a repulsive interaction of He with neighboring Re and W atoms. Specifically, the solution energies of He in bulk W are lower than that in W-Re system, implying the W-He repulsion is weaker than Re-He interaction. This is because the number of valence electrons for Re is larger than that for W. When the atomic distance of Re/W-He is larger than 2.25 Å, the solution energy difference converges to zero, suggesting that the Re-He interaction is same as W-He interaction.

3.1.2. Interaction of a single Re with He clusters in W

Next, we explore the interaction of a single Re with multi-He atoms by calculating their binding energies. Based on the most stable configuration of Re-He₁ (see Table 1) in W, the subsequent He atom is introduced one by one and set at different TISs surrounding Re to determine the most stable Re-He_n ($n = 1\sim6$) complexes.

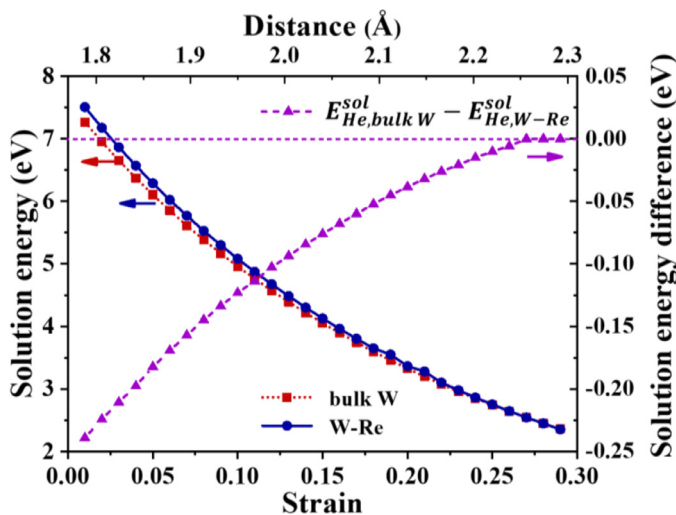


Fig. 1. The He solution energy in bulk W and W-Re system as well as their energy difference under hydrostatic strain. The distance means the 1NN distance of an interstitial He with W/Re atom in bcc W or W-Re system.

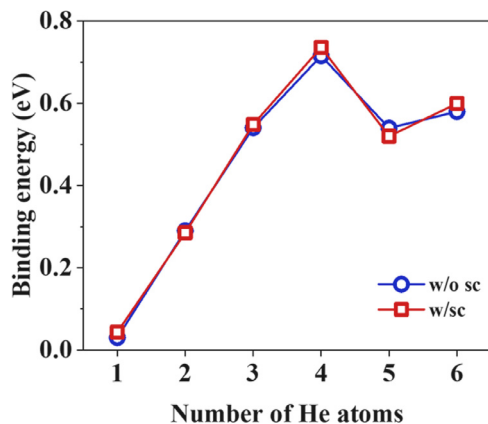


Fig. 2. The binding energy of Re with He clusters in W. The w/o sc and w/sc denote the calculation without and with 5p semi-core electrons, respectively.

The binding energies of Re and He clusters are defined as

$$E_{\text{He}}^b = E_{\text{W+Re}} + E_{\text{W+He}_n} - E_{\text{W+Re+He}_n} - E_{\text{W}}, \quad (2)$$

where $E_{\text{W+He}_n}$ and $E_{\text{W+Re+He}_n}$ are the energy of bulk W containing n interstitial He atoms without and with a substitutional Re atom. Positive binding energy denotes attractive interaction, while the negative value represents repulsion.

Fig. 2 illustrates the binding energies of Re with different He clusters in W. Since the multiple He atoms induce the large lattice distortion nearby (involving very short interatomic distances) and thus are sensitive to the core radius of the pseudopotential, the influence of semi-core electrons should be considered, as demonstrated in previous studies [48–51]. As illustrated in Fig. 2, it is found that the semi-core electrons have negligible effect on the binding energy of Re with He clusters in W. For example, the binding energy of He₂/He₃/He₄ with Re is 0.29/0.54/0.72 eV and 0.29/0.55/0.74 eV without and with semi-core electrons, respectively. These results suggest that the semi-core electrons can be neglected in the present work. Besides, it is important to note that the binding energies for Re and He clusters are always positive, indicating that there is attraction of Re with He clusters in W. Obviously, the binding energy between Re and He clusters in W is very sensitive to the number of He atoms, and the interaction between Re and He clusters is very different from that of Re with a single He. As displayed in Fig. 2, the binding energies of Re with He clus-

ters almost monotonically increase with the increasing numbers of He, from 0.03 eV for Re-He₁ to 0.72 eV for Re-He₄. After that, the binding energies of Re-He_n slight decrease for the case of He₅ and He₆, but the value is still above 0.5 eV. Apparently, these binding energies are much larger than that of Re-He₁, indicating that there is much stronger interaction between Re and He clusters in comparison with that between Re and a single He. Therefore, the attraction of Re-He_n is dramatically enhanced with the increasing of He numbers.

Interestingly, based on the atomic configuration in the vicinity of He clusters, the strong attraction between Re and He clusters in W can be attributed to two competing mechanisms, i.e. “He-dominated effect” for He₁/He₂ and “Re-dominated effect” for larger He clusters; both are important to understand the interaction of Re-He_n. For the “He-dominated effect”, although the dissolution of He in bulk W and W-Re systems induces the lattice expansion, the atomic configurations basically remain unchanged and distorted Re/W atoms still occupy the substitutional sites [see Fig. 3(a)–(c) and (i)–(k)]. In this case, the He-induced volume expansion in W-Re system is larger than that in bulk W (since the Re-W bonds in W-Re system are weaker than the W-W bonds in bulk), leading to the reduction of electron density and contributing to the attractive interaction of Re with He clusters. For the case of “Re-dominated effect”, the atomic configurations are substantially different. As displayed in Fig. 3(d)–(g) and (l)–(o), the He-induced lattice distortion is dramatically enhanced with the increasing of He numbers, and the distorted Re/W atom occupies interstitial position rather than the substitutional site. It can be found that the atomic distance of distorted Re (W) with its 1NN W is only 2.39 Å (2.41 Å) for He₄ cluster in W-Re system (bulk W), which is comparable with the 1NN Re-W (W-W) distance for interstitial Re (SIA) in bcc W [see Fig. 3(h) and (p)]. In this case, the He_n clusters in bulk W and W-Re systems can be partly equivalent to vacancy-He_n complex plus a self-interstitial atom and vacancy-He_n complex plus an interstitial Re atom, respectively. As reported in previous studies [49,52,53], the formation energy of an interstitial Re atom is much lower (~0.80 eV) than that of a SIA in W, and thus resulting in the attractive interaction between Re and He clusters. Therefore, with the increasing of He numbers, the He-induced distorted Re/W atom gradually transfers from the substitutional site into the interstitial site, and accordingly, the primary mechanisms responsible for the attraction between Re and He clusters transfer from “He-dominated mechanism” to “Re-dominated mechanism”.

3.1.3. Influence of a single Re atom on the mobility of He and He clusters in W

The migration of He plays a critical role on the microstructure evolution of W after He ions irradiation [54–56]. Here, we examine the migration of He and He clusters in W-Re system. Fig. 4 displays the migration energy barrier of a He atom in W with and without Re. Similar with previous studies [57,58], the migration energy barrier for He in W is 0.06 eV with the migration path of TIS→TIS. When a substitutional Re is introduced, two different migration paths are considered, including S₁→S₂ and S₂→S₃. As illustrated in Fig. 4, the migration energy barrier of S₁→S₂ and S₂→S₃ is 0.07 eV and 0.08 eV, respectively. These results are slightly higher than the migration energy barrier of He in W without Re, while the energy difference is no more than 0.02 eV. Thus, there is a weak suppressing effect of Re on the migration of a single He, owing to the weak attraction of Re-He₁ in W.

As shown in Section 3.1.2, the binding energy between Re and He clusters is much higher than that of Re-He₁, indicating the profound influence of Re on the He clusters migration. Nevertheless, to date the migration behaviors of He clusters in bcc W remain to be elucidated [59], and thus the direct investigation for the migration of He clusters in W-Re system is very difficult. To remedy this,

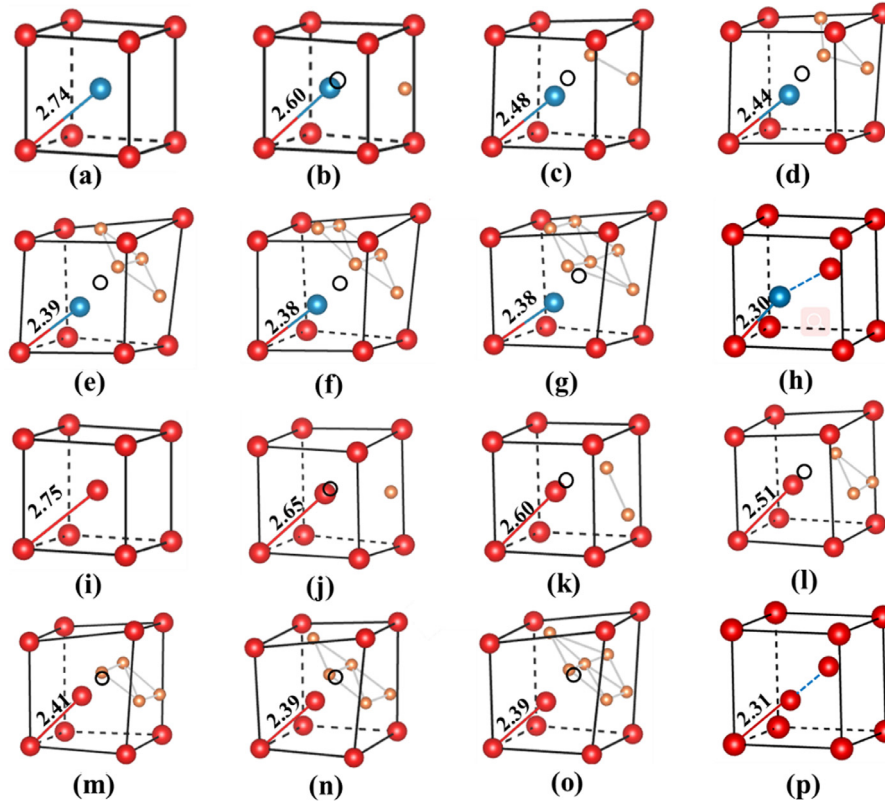


Fig. 3. The most stable configurations of He clusters in (a)-(h) W-Re system and (i)-(p) bulk W. For comparison, the atomic configuration of (h) an interstitial Re and (p) a self-interstitial atom in W are also given. The labels are the same as in Table 1.

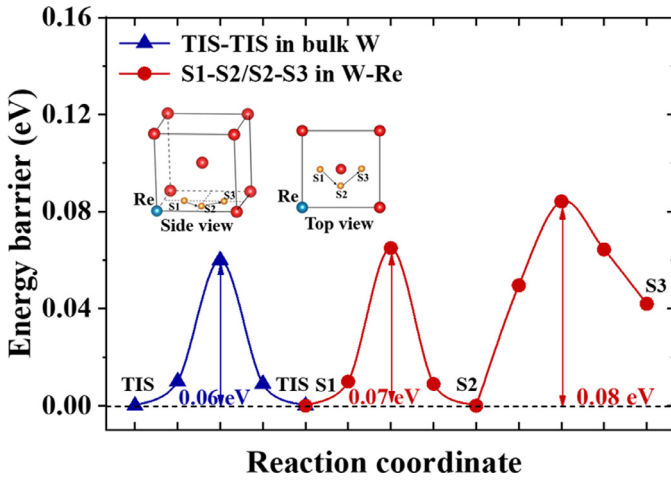


Fig. 4. The migration energy barriers and the corresponding migration paths of a single He atom in bulk W and W-Re system. The S1-S3 are the different TISs in the vicinity of a substitutional Re atom. The labels are the same as in Table 1.

we employ the classic McNabb-Foster formula to calculate the ratio of diffusivity between He clusters in W and He clusters in W-Re system [60–62]. The McNabb-Foster formula can be expressed as

$$D_{W-Re}^{He} = \frac{D_{pref}^{He}}{1 + c_{Re} \left(\frac{E_{Re-He}^b}{k_B T} \right)}, \quad (3)$$

where D_{pref}^{He} is the diffusivity of He clusters in bulk W. c_{Re} is the atomic concentration of Re and E_{Re-He}^b is the binding energy of Re-He_n. k_B is the Boltzmann constant and T is the temperature. Here, two different Re concentrations are considered, including 3 at.% and 10 at.%, which are consistent with the experiments [9,29].

As demonstrated in previous studies [47,48,63], there is a repulsive interaction between substitutional Re atoms in W, indicating the dispersed distribution of Re, and this repulsion becomes negligible when the Re-Re distance is larger than 3.17 Å. Hence, W-3 at.% Re (or W-10 at.% Re) can also be approximated as dilute-limit system (corresponding to our DFT calculations). This is also confirmed by previous study [64], in which the solution energy and migration energy barrier of H in 127W-1Re, 120W-8Re and 96W-32Re (Re atoms are distributed equably in W-Re lattice) are almost invariable. Based on the Eq. (3), the ratio of the diffusivity between He clusters in bulk W (D_{pref}^{He}) and He clusters in W-Re system (D_{W-Re}^{He}) is only dependent on the Re concentration and temperature.

Fig. 5 shows the ratio of the diffusivity for the different He clusters as a function of temperature. It can be found that the increase of Re concentration induces the decrease of the diffusivity ratios, but the variation trend is almost unchanged. Further, similar with the binding energy between Re and He in W, the diffusivity ratios are directly related to the number of He atoms. For a single He atom, the diffusivity ratio is almost invariable and equals to one at different temperature, suggesting the negligible effect of Re on the migration of a single He, which is due to the weak interaction of Re-He₁ in W. As for He clusters, the diffusivity ratio is less than one and decreased with the He numbers increasing. This indicates the suppressing of Re on the migration of He clusters in W and the suppressing effect is enhanced for the large He clusters. For example, with the addition of 10 at.% Re, the diffusivity ratio for He₂ cluster is 1.33×10^{-4} at room temperature (~300 K), while that for He₄ cluster is decreased to 9.49×10^{-12} . Also, the diffusivity ratio is increased with the increasing of temperature, and thus the suppressing effect of Re is mitigated at high temperature. This can be simply rationalized by the dissociation of Re-He_n at high temperature.

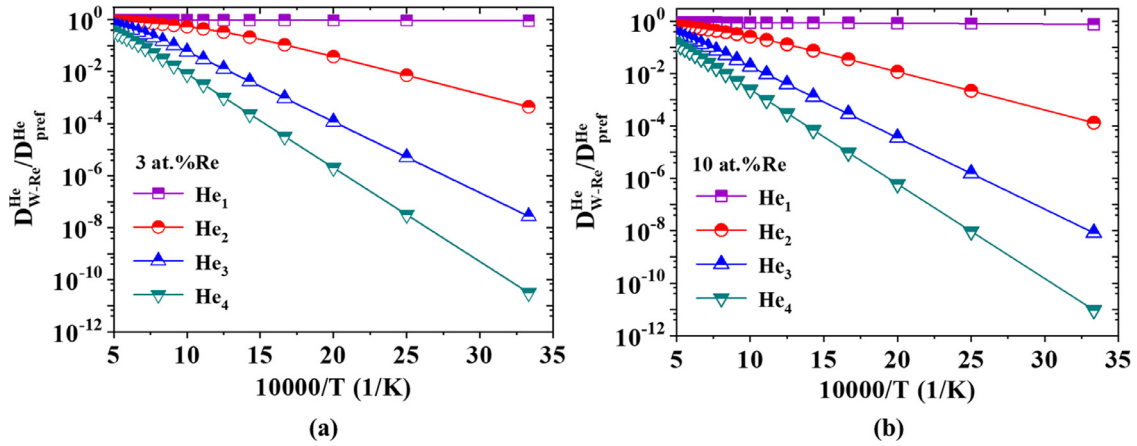


Fig. 5. The diffusivity ratio of He clusters ($D_{W-Re}^{He} / D_{W-Re}^{He_{pref}}$) in bulk W and W-Re system, (a) W-3 at.% Re and (b) W-10 at.% Re.

It is important to note that the possibility of a He atom dissociation from the clusters is neglected in Eq. (3). This can be attributed to the large gap between the dissociation energy and migration energy barrier of small He clusters in W. Based on our calculations, the dissociation energy (or sequential binding energy in the manuscript) of a He atom from He₂, He₃ and He₄ can reach up to 1.08 eV, 1.50 eV and 1.90 eV, respectively. However, as reported in previous studies, the migration energy barriers of small He clusters are extremely low (0.06–0.11 eV for He₂, 0.18–0.23 eV for He₃, 0.15–0.30 eV for He₄ in [59,65–67]), which are much lower than the dissociation energy. These results suggest that the probability of the dissociation of He clusters in W should be much lower than that of migration, and thus only plays a minor role on the evolution of He clusters in W. Indeed, these findings are consistent with previous molecular dynamic (MD) simulations [66,68,69], in which the migration and growth of He clusters dominate the evolution of He atoms in W from 100 K to 2500 K.

3.2. Interaction between Re-vacancy and multi-He atoms

As reported in previous studies [47,70,71], vacancy can serve as trapping center for both Re and He atoms in W, implying the formation of Re-vacancy-He (Re-V-He) complexes. Hence, taking Re₁-V, Re₄-V and Re₈-V as examples, we investigate the interaction of He with Re-V complexes in W by calculating the He trapping energy. The trapping energy of Re_m-V for He clusters can be expressed as

$$E_{He}^{trap} = E_{W+He_n} - E_W - E_{W+Re_m+V+He_n} + E_{W+Re_m+V}, \quad (4)$$

where $E_{W+Re_m+V+He_n}$ is the energy of bulk W containing a mono-vacancy, m (1 or 4 or 8) Re atoms and n He atoms. Positive trapping energy denotes attractive interaction, while the negative value represents repulsion.

Fig. 6 shows the total trapping energies of He clusters in the Re₁-V, Re₄-V and Re₈-V ($n = 1-5$) complexes. For comparison, the results of He in the mono-vacancy in W without Re are provided. Obviously, the He trapping energies are always positive, indicating the strong trapping capability of Re_m-V for He atoms. For the 1st He atom, the influence of Re atoms on its trapping energy in vacancy is negligible, as illustrated in Fig. 6. However, with the aggregation of He atoms, the influence of Re on the trapping of He in a mono-vacancy becomes stronger. As displayed in Fig. 6, although the trapping energies of He clusters in a mono-vacancy are almost the same as that in Re₁/Re₄-V complexes (except for He₅ clusters in Re₄-V), it is higher than that in Re₈-V. For instance, the trapping energy of He₂ cluster in Re₈-V complex is 6.42 eV, while that in a mono-vacancy, Re₁-V and Re₄-V complex can reach up to 6.80 eV,

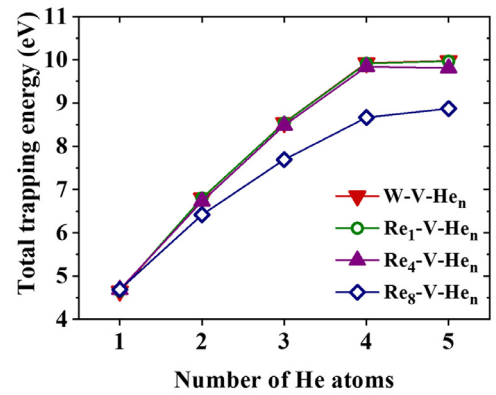


Fig. 6. The total trapping energy of He clusters in the mono-vacancy, Re₁-V, Re₄-V and Re₈-V.

6.80 eV, 6.73 eV, respectively. Similar variation trends of trapping energy are also observed for the He₃, He₄ and He₅ clusters, as presented in Fig. 6. These results suggest that the multiple Re atoms in W decrease the trapping capability of vacancy for He.

In order to elucidate the Re effects on the trapping capability of vacancy for He, the atomic configurations of He clusters in Re-V complexes are examined, as displayed in Fig. 7. For the case of 1st He atom, it energetically prefers to occupy the vacancy center in bulk W/W-Re systems [see Fig. 7(a)(f)(k)(p)], because the electron density at vacancy center ($\sim 0.025 e/\text{\AA}^3$) is much lower than that at other sites. In this case, the atomic distances of He with its 1NN Re/W atoms are as much as 2.75 Å, and thus the difference between Re-He and W-He interaction is almost negligible [see Fig. 1]. As the 2nd He added, two He atoms formed a dumbbell configuration along $\langle 111 \rangle$ direction with one 1NN Re/W atom, as shown in Fig. 7(b)(g)(l)(q). For a mono-vacancy and Re₁-V complex, the distance of 1NN W-He is much lower than that of Re-He (> 2.25 Å), corresponding to the same trapping energy of He₂ [see Fig. 6]. For the case of a Re₄-V complex, although the distance of Re-He is lower than that W-He (only for one He atom), it can reach up to 2.30 Å, resulting in the negligible effect on He trapping energy. As for the Re₈-V complex, the 1NN distance of He with neighboring Re is only 2.07 Å. At this distance, the Re-He repulsion is stronger than W-He repulsion [see Fig. 1], leading to the increase of solution energy and decrease of trapping energy for He in Re₈-V. Similar results are also observed for He₃, He₄ and He₅ clusters, in which the trapping energy of He clusters can be rationalized by the 1NN distance between He and Re atoms.

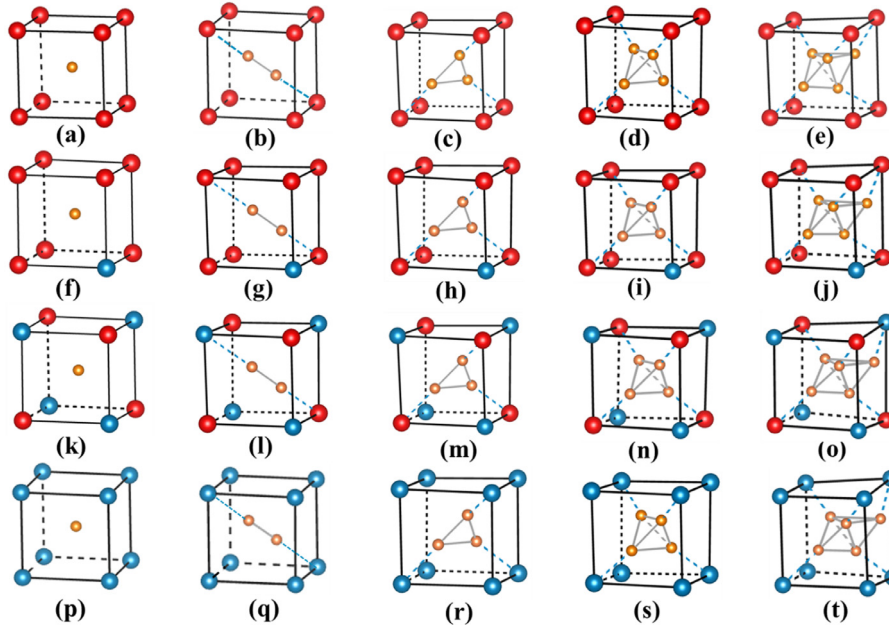


Fig. 7. The most stable configurations of He clusters in the (a)–(e) mono-vacancy (f)–(j) $\text{Re}_1\text{-V}$ (k)–(o) $\text{Re}_4\text{-V}$ and (p)–(t) $\text{Re}_8\text{-V}$. Blue dotted lines connect the He atom and its neighboring Re/W atoms. The labels are the same as in [table 1](#).

3.3. Behaviors of He in Re-rich precipitates (W-Re σ phase)

According to the phase diagrams of W-Re alloys [72,73], the solubility limit of Re in W under thermal equilibrium condition can reach up to 26 at.% at 1500 K. However, the high-energy particles irradiation will induce the aggregation of Re atoms and the formation of Re-rich precipitates in W, known as “radiation-induced precipitation (RIP)”. Generally, due to the different atomic configuration, the evolution of interstitial solutes in Re-rich precipitates should be completely different from that in bcc system [42]. Therefore, a full investigation of the He behaviors in Re-rich precipitates is of great importance to understand the effect of Re on the performance of W.

3.3.1. Dissolution of He in σ phase

Here, we only consider the most stable configuration of W-Re σ phase (W-33.3 at.%Re, see more detail in Ref. [42]). As demonstrated in our previous study [42], there are two types of interstitial sites in σ phase, including the tetrahedral sites [see [Fig. 8\(a\)](#)] and trigonal sites [see [Fig. 8\(b\)](#)]. Then, a single He atom is set at potential interstitial sites and the corresponding He solution energies are examined in σ phase. Here, the solution energies of He can be obtained by

$$E_{\text{He}}^{\text{sol}} = E_{\sigma+\text{He}} - E_{\sigma} - E_{\text{He}}^{\text{ref}}, \quad (5)$$

where $E_{\sigma+\text{He}}$ and E_{σ} are the energy of systems with and without an interstitial He atom in σ phase, respectively. The He solution energies at potential interstitial sites in σ phase are shown in [Table 2](#). It should be noted that some interstitial sites are unstable for He, and thus the He solution energy at these sites are not presented. As seen in [Table 2](#), the He solution energy is strongly related to the He-occupied site, since the energy differences at different interstitial sites can reach up to 2.14 eV. Specifically, the solution energies of He at most interstitial sites ($\sim 64\%$ of all possible sites) in σ phase are lower than that in perfect W (~ 6.31 eV). Further, the most stable occupation of He in σ phase is *tri1* site with the solution energy of 4.80 eV. Therefore, the formation of W-Re σ phase will enhance the dissolution of He in W.

To understand the stability of He in W-Re σ phase, the He solution energies are also divided into EC and MC (see more detail in

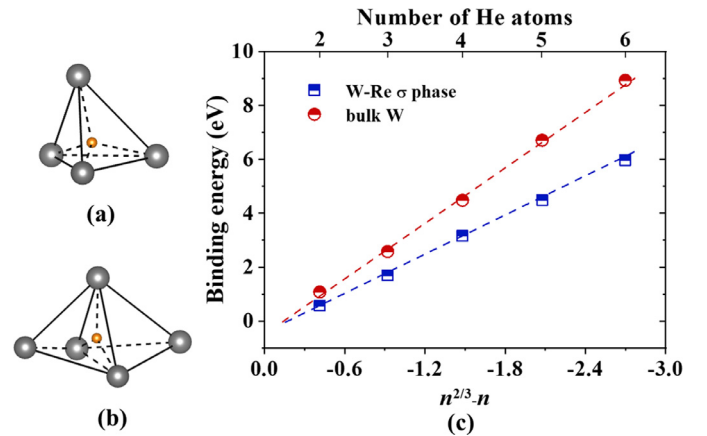


Fig. 8. (a)(b) The local atomic structure of *tet* and *tri* site in W-Re σ phase. The gray balls represent neighboring host (W or Re) atoms surrounding the interstitial He atoms (yellow balls). (c) The binding energy of He clusters in W-Re σ phase and bulk W, following a universal scaling relation with the cluster size, $E_b \propto (n^{2/3} - n)$. (For interpretation of the references to colour in this figure legend, the reader is referred to the web version of this article.)

[Section 3.1.1](#)). As presented in [Table 2](#), the MC is much lower than EC for He in σ phase, suggesting the poor solubilities of He in σ phase is mainly controlled by the electronic interaction of He with neighboring Re/W atoms. More importantly, the EC dominates the reduction of He solution energies from bulk W to σ phase. For example, the EC and MC of He at *tri1* site in σ phase is 3.81 eV and 0.99 eV, while that at TIS in bulk W is 5.24 eV and 1.07 eV [see [Table 1](#)] respectively. Hence, the difference of EC can reach up to 1.43 eV, which is much higher than the MC difference (~ 0.08 eV).

As mentioned in [Section 3.1.1](#), the EC for He solution energy in metals is closely related to the electron density of He-occupied position, and thus the electron densities of He are also calculated in [Table 2](#). Obviously, the electron densities of He-occupied position in σ phase are lower than that in perfect W ($\sim 0.176 \text{ e}/\text{\AA}^3$), which is basically consistent with the variation of EC. Intriguingly, the difference of electron density can be well interpreted by the atomic

Table 2

The solution energy (E_{sol} , eV), MC (eV) and EC (eV) of He at possible interstitial sites (*tet* and *tri*) in W-33.3 at.%Re σ phase. The corresponding local atomic environments are presented. Four W/Re in *tet* denote the 1NN host atoms for interstitial He, while five W/Re in *tri* denote the 1NN (first three) and 2NN (latter two) host atoms for He. The electron densities (ρ_e^{He} , $e/\text{\AA}^3$) of He at different interstitial sites and the 1NN average distances ($d_{Re/W-He}$, \AA) of Re/W-He are also presented.

Interstitial site	Position	Local structure	E_{sol}	MC	EC	ρ_e^{He}	$d_{Re/W-He}$
<i>tet</i>	1	WWWW	4.82	0.97	3.85	0.122	2.05
	2	WWWW	4.97	0.88	4.09	0.128	2.01
	3	WWWRe	5.53	1.24	4.29	0.150	1.98
	4	WReReRe	5.64	1.65	3.99	0.113	2.07
	5	WWReRe	6.62	1.49	5.13	0.197	1.88
	6	WWReRe	6.69	1.48	5.21	0.206	1.87
<i>tri</i>	1	WWWWWW	4.80	0.99	3.81	0.123	2.01
	2	WWReWW	5.09	1.59	3.50	0.125	1.97
	3	WWReWW	5.85	1.75	4.10	0.164	1.85
	4	WWReReRe	6.89	1.49	5.40	0.198	1.81
	5	ReReReWW	6.94	2.25	4.69	0.181	1.80

configuration. As illustrated in Table 2, the 1NN average distance between He and neighboring Re/W atoms at *tri1* site is 2.01 \AA , while that at TIS in perfect W is only 1.94 \AA . Such remarkable variation of atomic distance suggests that the σ phase has large available volumes at interstitial sites in comparison with bulk W, which reduces the electron density of He-occupied position and increases the solubility of He.

3.3.2. Clustering of He atoms in σ phase

Moreover, spontaneous aggregation of He in metals is a well-documented phenomenon, known as self-trapping [45,46,74]. Here, to determine the self-trapping behaviors of He in σ phase, we calculate the binding energy of He clusters, which can be obtained by

$$E_{He}^b = nE_{\sigma+He} - E_{\sigma+He_n} - (n-1)E_{\sigma}, \quad (6)$$

where $E_{\sigma+He_n}$ is the energy of σ phase system including n interstitial He atoms.

The binding energies of He clusters in σ phase and bulk W are illustrated in Fig. 8(c). It is found that the binding energy is positive for all cases, indicating the self-trapping of He atoms. With the increasing of He numbers, the binding energy of He clusters increases in σ phase, from 0.57 eV for He₂ cluster to 5.90 eV for He₆ cluster. Hence, the stability of He clusters is dramatically enhanced by the spontaneous aggregation of He atoms. Besides, the binding energies of He clusters in σ phase are always lower in comparison with that in bulk W at the same number of He atoms. For example, the binding energy of He₄ cluster is only 3.16 eV in σ phase, while that in bulk W can reach up to 4.48 eV. Thus, the self-trapping of He in bulk W is more favorable than that in σ phase. In our previous study [45], we proposed a model of electrophobic interaction, which can be used to interpret the He self-trapping in metals. Within this concept, the binding energy of He clusters in pure metals follows a universal law scaling with the He numbers, i.e. $E_b \propto (n^{2/3} - n)$. As displayed in Fig. 8(c), the binding energy of He clusters in σ phase also follows the same universal law as that of He clusters in W, which monotonically increases with the decreasing of $(n^{2/3} - n)$. However, the absolute value of curve slope for He in bulk W (~ 3.56) is much higher than that in σ phase (~ 2.42), indicating that the electrophobic interaction of He in bulk W is stronger than that in σ phase. This can be attributed to the variation of electronic environment, because the electron density at TIS in bulk W ($\sim 0.176 \text{ e}/\text{\AA}^3$) is higher than that at *tri1* in σ phase ($\sim 0.123 \text{ e}/\text{\AA}^3$). Also, it is interesting to note the ratio of the electron density ($0.176/0.123 = 1.35$) is comparable with the ratio of curve slope ($3.56/2.42 = 1.47$), confirming that the electrophobic interaction is originated from the repulsion between He and electron environment.

3.4. Influence of Re on He behaviors in W

Indeed, the influence of Re on He behaviors in W have been explored both computationally [31–34] and experimentally [9,29,30]. However, since the interaction of Re with a single He in W is extremely weak based on the DFT calculations [31,34], the physical origin responsible for the experimental observed influence of Re on the He-induced surface morphology in W is still unclear. In present work, it is found that the interaction between Re and He clusters are substantially different with that between Re and a single He atom. There are strong attractive interactions of Re with He clusters in W, and these interactions are dramatically enhanced with the increasing of He numbers. For example, the binding energy of Re-He₁ is only 0.03 eV, while that of Re-He₂ and Re-He₄ can reach up to 0.29 eV and 0.72 eV, respectively. Further, such strong attractions indicate that the substitutional Re atom is a strong trapping center for interstitial He atoms, and thus effectively reducing the mobility of He clusters in W. In order to verify this speculation, the pinning effects of Re on the migration of He clusters is evaluated by McNabb-Foster formula [see Eq. (3)], in which the temperature effects are also considered. As illustrated in Fig. 5, the pinning effects of Re on the migration of He clusters is enhanced with the decreasing of temperature. For example, with the addition of 3 at.% Re, the diffusivity ratios for He₂, He₃ and He₄ is 8.02×10^{-1} , 3.98×10^{-1} and 1.57×10^{-1} at 1600 K, while that is decreased to 2.99×10^{-1} , 9.87×10^{-3} and 2.17×10^{-10} at 773 K. Hence, the addition of Re can significantly reduce the mobility of small He clusters in temperature ranges relevant to experiments (773–1600 K in [9,29,30]). Generally, it is believed that the formation of He-induced damage (e.g. fuzz) is closely related to the growth of He clusters in metals [75–80], which is controlled by the migration of small He clusters. Therefore, owing to the strong attraction between Re and He clusters, the presence of Re suppresses the migration of He clusters, and thus inhibiting the growth of He-induced damage in W. These findings provide a reasonable interpretation for the microstructure evolution of W-Re alloys under He plasma irradiation [9,29].

It should be noted that the irradiation of high-energy particles will induce the aggregation of Re atoms, leading to the formation of Re clusters and Re-rich precipitates. Hence, the interaction of Re clusters with He in bcc W and the He behaviors in Re-rich precipitates (W-Re σ phase) are also investigated. The trapping capability of vacancy for He is stronger than that of Re_m-vacancy in W, and thus the clustering of Re atoms reduces the He/vacancy ratios in He-vacancy complexes. This is consistent with recent experimental observations, in which the internal pressure of He bubbles in W-Re alloys is lower than that in pure W, i.e. the lower He/vacancy ratio for bubbles [30]. Further, the presence of W-Re σ phase has significant effects on the behaviors of He in W-Re system. It should be noted that although the boundaries between W-Re σ phase and

BCC phase may provide the strong trapping sites for He, this effect is not considered in the present work. This is because that the size of radiation-induced Re-rich precipitates in W can reach up to ~100 nm after neutron irradiation of ~2 dpa at 923 K in the High Flux Isotope Reactor (HFIR) [81]. Such large size of Re-rich precipitates indicates that the bulk system of σ phase also plays a critical role on the behaviors of He in W-Re system, especially at high irradiation level (since the size of Re-rich precipitates increases with the increasing of irradiation dose). Hence, as the initial study of this topic, we focused on behaviors of He in bulk system (both solid-solution BCC phase and Re-rich σ phase). According to our calculations, the He behaviors in σ phase is significantly different with that in bcc system. Although the binding energy of He clusters in bulk W is higher than that in W-Re σ phase, the solution energies of He at most interstitial positions (~64%) in σ phase are lower than that in bulk W. More importantly, the segregation energy of He clusters from bulk W to W-Re σ phase is positive for all cases and increases with the increasing of He numbers, from 2.36 eV for He₂ to 4.43 eV for He₄. These results suggest that the He clusters energetically prefer to segregate from bcc W to W-Re σ phase, which increases the He retention and affects the responses of W to He-induced damage. Although the effect of Re-rich phase on the performance of W after He plasma irradiation is still unclear in experiments, this speculation is confirmed by the studies of other W-based alloys. For example, the thickness of coral-like structures (a mixture of fuzzy and deep holes) in vanadium-rich region is significantly higher as compared with W-rich region and solid-solution W-vanadium region [23], implying the negative effects of vanadium-rich region on the properties of W.

4. Conclusion

By employing the first-principles calculation and thermodynamic model, we have systematically investigated the influence of Re on the He behaviors in W with different distribution of Re. It is found that the interaction of a single Re with an interstitial He is extremely weak, which means the negligible influence of Re on a single He atom in W. More importantly, with the increasing of He cluster size, the binding energies of Re with He clusters increase rapidly, from 0.03 eV for Re-He₁ to 0.72 eV for Re-He₄. Such large difference can be attributed to the large lattice distortion induced by He clusters, which reduces the electron density of He-occupied position and induces the transition of neighboring Re/W atom from a substitutional site to an interstitial site. Specifically, due to the strong attraction between Re and He clusters, the Re atoms have a pinning effect on the mobility of He clusters, and thus inhibiting the growth of He-induced damage in W. Moreover, the aggregation of Re atom weakens the trapping capability of vacancy for He atom, leading to the decrease of He/vacancy ratio in He-vacancy complexes. These findings give a plausible interpretation for the experimental observed influence of Re on the He-induced morphology in W. Further, we have determined the behaviors of He in Re-rich phases (W-Re σ phase). The He solution energies at ~64% interstitial sites in σ phase are lower compared with that at TIS in bulk W, and the self-trapping of He is also observed in σ phase. Hence, the W-Re σ phase can serve as the trapping center for He atoms, enhancing the formation of He clusters and aggravating the He-induced damage in W. Our calculations reveal a critical role of Re distribution on the He clusters evolution in W and deepen our understanding of the He behaviors in W-based alloys.

Declaration of Competing Interest

The authors declare that they have no known competing financial interests or personal relationships that could have appeared to influence the work reported in this paper.

CRediT authorship contribution statement

Fang-Ya Yue: Investigation, Writing - original draft. **Yu-Hao Li:** Methodology, Resources, Writing - review & editing. **Qing-Yuan Ren:** Methodology, Formal analysis. **Fang-Fei Ma:** Visualization, Validation. **Zhong-Zhu Li:** Visualization, Formal analysis. **Hong-Bo Zhou:** Conceptualization, Writing - review & editing, Supervision, Funding acquisition. **Huiqiu Deng:** Writing - review & editing. **Ying Zhang:** Resources, Formal analysis. **Guang-Hong Lu:** Formal analysis, Writing - review & editing, Funding acquisition.

Acknowledgements

This research is supported by the National Key R&D Program of China with Grant Nos. 2018YFE0308103 and the National Natural Science Foundation of China with Grant Nos. 11675011.

References

- [1] H. Bolt, V. Barabash, G. Federici, J. Linke, A. Loarte, J. Roth, K. Sato, Plasma facing and high heat flux materials - Needs for ITER and beyond, *J. Nucl. Mater.* 307–311 (2002) 43–52.
- [2] R. Causey, K. Wilson, T. Venhaus, W.R. Wampler, Tritium retention in tungsten exposed to intense fluxes of 100eV tritons, *J. Nucl. Mater.* 266 (1999) 467–471.
- [3] W.M. Shu, E. Wakai, T. Yamanishi, Blister bursting and deuterium bursting release from tungsten exposed to high fluxes of high flux and low energy deuterium plasma, *Nucl. Fusion* 47 (2007) 201.
- [4] J. Roth, E. Tsiatroni, A. Loarte, T. Loarer, G. Counsell, R. Neu, V. Philipps, S. Brezinsek, M. Lehnen, P. Coad, C. Grisolia, K. Schmid, K. Krieger, A. Kallenbach, B. Lipschultz, R. Doerner, R. Causey, V. Alimov, W. Shu, O. Ogorodnikova, A. Kirschner, G. Federici, A. Kukushkin, Recent analysis of key plasma wall interactions issues for ITER, *J. Nucl. Mater.* 390–391 (2009) 1–9.
- [5] A. El-Kharbachi, J. Chêne, S. Garcia-Argote, L. Marchetti, F. Martin, F. Misserque, D. Vrel, M. Redolfi, V. Malard, C. Grisolia, B. Rousseau, Tritium absorption/desorption in ITER-like tungsten particles, *Int. J. Hydrogen Energy* 39 (2014) 10525–10536.
- [6] H. Iwakiri, K. Yasunaga, K. Morishita, N. Yoshida, Microstructure evolution in tungsten during low-energy helium ion irradiation, *J. Nucl. Mater.* 283–287 (2000) 1134–1138.
- [7] Q. Xu, N. Yoshida, T. Yoshiie, Accumulation of helium in tungsten irradiated by helium and neutrons, *J. Nucl. Mater.* 367–370 (2007) 806–811.
- [8] S. Kajita, W. Sakaguchi, N. Ohno, N. Yoshida, T. Saeki, Formation process of tungsten nanostructure by the exposure to helium plasma under fusion relevant plasma conditions, *Nucl. Fusion* 49 (2009) 095005.
- [9] M.J. Baldwin, R.P. Doerner, Formation of helium induced nanostructure “fuzz” on various tungsten grades, *J. Nucl. Mater.* 404 (2010) 165–173.
- [10] M. Thompson, D. Drummond, J. Sullivan, R. Elliman, P. Kluth, N. Kirby, D. Riley, C.S. Corr, Effect of W self-implantation and He plasma exposure on early-stage defect and bubble formation in tungsten, *Nucl. Fusion* 58 (2018) 066010.
- [11] M. Miyamoto, D. Nishijima, Y. Ueda, R.P. Doerner, H. Kurishita, M.J. Baldwin, S. Morito, K. Ono, J. Hanna, Observations of suppressed retention and blistering for tungsten exposed to deuterium-helium mixture plasmas, *Nucl. Fusion* 49 (2009) 065035.
- [12] K. Farrell, P. J. Maziasz, E. H. Lee, L.K. Mansur, Modification of radiation damage microstructure by helium, *Radiat. Eff.* 78 (1983) 277–295.
- [13] H. Ullmaier, The influence of helium on the bulk properties of fusion reactor structural materials, *Nucl. Fusion* 24 (1984) 1039–1083.
- [14] H. Trinkaus, B.N. Singh, Helium accumulation in metals during irradiation - where do we stand? *J. Nucl. Mater.* 323 (2003) 229–242.
- [15] S. Cui, M. Simmonds, W. Qin, F. Ren, G.R. Tynan, R.P. Doerner, R. Chen, Thermal conductivity reduction of tungsten plasma facing material due to helium plasma irradiation in PISCES using the improved 3-omega method, *J. Nucl. Mater.* 486 (2017) 267–273.
- [16] S. Kajita, T. Yagi, K. Kobayashi, M. Tokitani, N. Ohno, Measurement of thermophysical property of plasma forming tungsten nanofiber layer, *Jpn. J. Appl. Phys.* 55 (2016) 056203.
- [17] K.O.E. Henriksson, K. Nordlund, A. Krashennikov, J. Keinonen, Difference in formation of hydrogen and helium clusters in tungsten, *Appl. Phys. Lett.* 87 (2005) 163113.
- [18] Y. Noiri, S. Kajita, N. Ohno, Nanostructure growth by helium plasma irradiation to tungsten in sputtering regime, *J. Nucl. Mater.* 463 (2015) 285–288.
- [19] M.R. Gilbert, S.L. Dudarev, S. Zheng, L.W. Packer, J.C. Sublet, An integrated model for materials in a fusion power plant: transmutation, gas production, and helium embrittlement under neutron irradiation, *Nucl. Fusion* 52 (2012) 083019.
- [20] S. Wurster, B. Gludovatz, A. Hoffmann, R. Pippan, Fracture behaviour of tungsten-vanadium and tungsten-tantalum alloys and composites, *J. Nucl. Mater.* 413 (2011) 166–176.
- [21] Y. Mutoh, K. Ichikawa, K. Nagata, M. Takeuchi, Effect of rhenium addition on fracture toughness of tungsten at elevated temperatures, *J. Mater. Sci.* 30 (1995) 770–775.

- [22] H. Kurishita, Y. Amano, S. Kobayashi, K. Nakai, H. Arakawa, Y. Hiraoka, T. Takida, K. Takebe, H. Matsui, Development of ultra-fine grained W-TiC and their mechanical properties for fusion applications, *J. Nucl. Mater.* 367–370 (2007) 1453–1457.
- [23] J. Wang, C. Li, Y. Yuan, H. Greuner, L. Cheng, G.H. Lu, Surface modification of W-V alloy exposed to high heat flux helium neutral beams, *Nucl. Fusion* 58 (2018) 096001.
- [24] L. Romaner, C. Ambrosch-Draxl, R. Pippin, Effect of rhenium on the dislocation core structure in tungsten, *Phys. Rev. Lett.* 104 (2010) 195503.
- [25] I. Smid, M. Akiba, G. Vieider, I. Plochl, Development of tungsten armor and bonding to copper for plasma-interactive components, *J. Nucl. Mater.* 258–263 (1998) 160–172.
- [26] X. Hu, T. Koyanagi, M. Fukuda, N.A.P.K. Kumar, L.L. Snead, B.D. Wirth, Y. Katoh, Irradiation hardening of pure tungsten exposed to neutron irradiation, *J. Nucl. Mater.* 480 (2016) 235–243.
- [27] M. Fukuda, T. Tanno, S. Nogami, A. Hasegawa, Effects of Re content and fabrication process on microstructural changes and hardening in neutron irradiated tungsten, *Mater. Trans.* 53 (2012) 2145–2150.
- [28] D.E.J. Armstrong, X. Yi, E.A. Marquis, S.G. Roberts, Hardening of self ion implanted tungsten and tungsten 5-wt% rhenium, *J. Nucl. Mater.* 432 (2013) 428–436.
- [29] A. Khan, G. De Temmerman, T.W. Morgan, M.B. Ward, Effect of rhenium addition on tungsten fuzz formation in helium plasmas, *J. Nucl. Mater.* 474 (2016) 99–104.
- [30] X. Yi, K. Arakawa, F. Ferroni, M.L. Jenkins, W. Han, P. Liu, F. Wan, High-temperature damage evolution in 10 keV He⁺ irradiated W and W-5Re, *Mater. Charact.* 145 (2018) 77–86.
- [31] X. Wu, X.S. Kong, Y.W. You, C.S. Liu, Q.F. Fang, J.L. Chen, G.N. Luo, Z. Wang, Effects of alloying and transmutation impurities on stability and mobility of helium in tungsten under a fusion environment, *Nucl. Fusion* 53 (2013) 073049.
- [32] X. Wu, X.S. Kong, Y.W. You, C.S. Liu, Q.F. Fang, J.L. Chen, G.N. Luo, Z. Wang, First principles study of helium trapping by solute elements in tungsten, *J. Nucl. Mater.* 455 (2014) 151–156.
- [33] Y.W. You, J. Sun, X. Wu, Y. Xu, T. Zhang, T. Hao, Q.F. Fang, C.S. Liu, Interplay of solute-mixed self-interstitial atoms and substitutional solutes with interstitial and substitutional helium atoms in tungsten-transition metal alloys, *Nucl. Fusion* 59 (2019) 026002.
- [34] C.S. Becquart, C. Domain, U. Sarkar, A. Debacker, M. Hou, Microstructural evolution of irradiated tungsten: ab initio parameterisation of an OKMC model, *J. Nucl. Mater.* 403 (2010) 75–88.
- [35] P.E. Blöchl, Projector augmented-wave method, *Phys. Rev. B* 50 (1994) 17953–17979.
- [36] G. Kresse, J. Furthmüller, Efficient iterative schemes for ab initio total-energy calculations using a plane-wave basis set, *Phys. Rev. B* 54 (1996) 11169–11186.
- [37] J.P. Perdew, K. Burke, M. Ernzerhof, Generalized gradient approximation made simple, *Phys. Rev. Lett.* 77 (1996) 3865–3868.
- [38] J. Gotch, A climbing image nudged elastic band method for finding saddle points and minimum energy paths, *J. Chem. Phys.* 113 (2006) 9901–9904.
- [39] I.K. Suh, H. Ohta, Y. Waseda, High-temperature thermal expansion of six metallic elements measured by dilatation method and X-ray diffraction, *J. Mater. Sci.* 23 (1988) 757–760.
- [40] X.G. Lu, M. Selleby, B. Sundman, Assessments of molar volume and thermal expansion for selected bcc, fcc and hcp metallic elements, *CALPHAD* 29 (2005) 68–89.
- [41] C.G. Wilson, Order in binary σ -phases, *Acta Crystallogr.* 16 (1963) 724–730.
- [42] F.-Y. Yue, Y.-H. Li, H.-B. Zhou, Y. Zhang, G.-H. Lu, Insight into the enhancement effect of rhenium-rich precipitation on hydrogen retention in tungsten by investigating the behaviors of hydrogen in tungsten-rhenium sigma phase, *Int. J. Hydrogen Energy* 44 (2019) 24880–24894.
- [43] H.B. Zhou, Y.L. Liu, S. Jin, Y. Zhang, G.N. Luo, G.H. Lu, Towards suppressing H blistering by investigating the physical origin of the H-He interaction in W, *Nucl. Fusion* 50 (2010) 115010.
- [44] Y.W. You, J. Hou, J. Sun, X.S. Kong, X. Wu, C.S. Liu, J.L. Chen, The behaviors of helium atoms in tantalum, rhenium and osmium, *J. Nucl. Mater.* 499 (2018) 1–8.
- [45] H.B. Zhou, J.L. Wang, W. Jiang, G.H. Lu, J.A. Aguiar, F. Liu, Electrophobic interaction induced impurity clustering in metals, *Acta Mater.* 119 (2016) 1–8.
- [46] Y.H. Li, H.B. Zhou, G.H. Lu, Towards understanding the strong trapping effects of noble gas elements on hydrogen in tungsten, *Int. J. Hydrogen Energy* 42 (2017) 6902–6917.
- [47] Y.H. Li, H.B. Zhou, S. Jin, Y. Zhang, H. Deng, G.H. Lu, Behaviors of transmutation elements Re and Os and their effects on energetics and clustering of vacancy and self-interstitial atoms in W, *Nucl. Fusion* 57 (2017) 046006.
- [48] X.S. Kong, X. Wu, Y.W. You, C.S. Liu, Q.F. Fang, J.L. Chen, G.N. Luo, Z. Wang, First-principles calculations of transition metal-solute interactions with point defects in tungsten, *Acta Mater.* 66 (2014) 172–183.
- [49] L. Gharaee, P. Erhart, A first-principles investigation of interstitial defects in dilute tungsten alloys, *J. Nucl. Mater.* 467 (2015) 448–456.
- [50] L. Ventelon, F. Willaime, C.C. Fu, M. Heran, I. Ginoux, Ab initio investigation of radiation defects in tungsten: structure of self-interstitials and specificity of di-vacancies compared to other bcc transition metals, *J. Nucl. Mater.* 425 (2012) 16–21.
- [51] W. Setyawan, G. Nandipati, R.J. Kurtz, Ab initio study of interstitial cluster interaction with Re, Os, and Ta in W, *J. Nucl. Mater.* 484 (2017) 30–41.
- [52] Y.H. Li, H.B. Zhou, H. Deng, G. Lu, G.H. Lu, Towards understanding the mechanism of rhenium and osmium precipitation in tungsten and its implication for tungsten-based alloys, *J. Nucl. Mater.* 505 (2018) 30–43.
- [53] T. Suzudo, M. Yamaguchi, A. Hasegawa, Stability and mobility of rhenium and osmium in tungsten: first principles study, *Model. Simul. Mater. Sci. Eng.* 22 (2014) 075006.
- [54] N. Yoshida, H. Iwakiri, K. Tokunaga, T. Baba, Impact of low energy helium irradiation on plasma facing metals, *J. Nucl. Mater.* 337–339 (2005) 946–950.
- [55] D. Perez, L. Sandoval, S. Blondel, B.D. Wirth, B.P. Uberuaga, A.F. Voter, The mobility of small vacancy/helium complexes in tungsten and its impact on retention in fusion-relevant conditions, *Sci. Rep.* 7 (2017) 2522.
- [56] Q. Yang, Y.W. You, L. Liu, H. Fan, W. Ni, D. Liu, C.S. Liu, G. Benstetter, Y. Wang, Nanostructured fuzz growth on tungsten under low-energy and high-flux He irradiation, *Sci. Rep.* 5 (2015) 10959.
- [57] C.S. Becquart, C. Domain, Migration energy of He in W revisited by Ab initio calculations, *Phys. Rev. Lett.* 97 (2006) 196402.
- [58] Y.H. Li, H.B. Zhou, S. Jin, Y. Zhang, G.H. Lu, Strain-induced variation of electronic structure of helium in tungsten and its effects on dissolution and diffusion, *Comput. Mater. Sci.* 95 (2014) 536–539.
- [59] J.L. Cao, W.T. Geng, Migration of helium-pair in metals, *J. Nucl. Mater.* 478 (2016) 13–25.
- [60] R.A. Oriani, The diffusion and trapping of hydrogen in steel, *Acta Metall.* 18 (1970) 147–157.
- [61] Y. Kadim, M. Gamba, M. Faïd, Identification of the hydrogen diffusion parameters in bearing steel by evolutionary algorithm, *J. Alloys Compd.* 705 (2017) 475–485.
- [62] X.S. Kong, S. Wang, X. Wu, Y.W. You, C.S. Liu, Q.F. Fang, J.L. Chen, G.N. Luo, First-principles calculations of hydrogen solution and diffusion in tungsten: temperature and defect-trapping effects, *Acta Mater.* 84 (2015) 426–435.
- [63] W.L. Yan, H.B. Zhou, S. Jin, Y. Zhang, G.H. Lu, Dissolution energetics and its strain dependence of transition metal alloying elements in tungsten, *J. Nucl. Mater.* 456 (2015) 260–265.
- [64] F. Ren, W. Yin, Q. Yu, X. Jia, Z. Zhao, B. Wang, Solution and diffusion of hydrogen isotopes in tungsten-rhenium alloy, *J. Nucl. Mater.* 491 (2017) 206–212.
- [65] X.C. Li, X. Shu, P. Tao, Y. Yu, G.J. Niu, Y. Xu, F. Gao, G.N. Luo, Molecular dynamics simulation of helium cluster diffusion and bubble formation in bulk tungsten, *J. Nucl. Mater.* 455 (2014) 544–548.
- [66] Y.L. Zhou, J. Wang, Q. Hou, A.H. Deng, Molecular dynamics simulations of the diffusion and coalescence of helium in tungsten, *J. Nucl. Mater.* 446 (2014) 49–55.
- [67] F. Zhou, J. Fang, H. Deng, J. Liu, S. Xiao, X. Shu, F. Gao, W. Hu, New interatomic potentials for studying the behavior of noble gas atoms in tungsten, *J. Nucl. Mater.* 467 (2015) 398–405.
- [68] L. Sandoval, D. Perez, B.P. Uberuaga, A.F. Voter, Competing kinetics and bubble morphology in W, *Phys. Rev. Lett.* 114 (2015) 1–5.
- [69] D. Perez, T. Vogel, B.P. Uberuaga, Diffusion and transformation kinetics of small helium clusters in bulk tungsten, *Phys. Rev. B* 90 (2014) 014102.
- [70] J.S. Wróbel, D. Nguyen-Manh, K.J. Kurzydowski, S.L. Dudarev, A first-principles model for anomalous segregation in dilute ternary tungsten-rhenium-vacancy alloys, *J. Phys. Condens. Matter* 29 (2017) 145403.
- [71] Y.W. You, X.S. Kong, X. Wu, C.S. Liu, Q.F. Fang, J.L. Chen, G.N. Luo, Clustering of transmutation elements tantalum, rhenium and osmium in tungsten in a fusion environment, *Nucl. Fusion* 57 (2017) 086006.
- [72] M. Ekman, K. Persson, G. Grimvall, Phase diagram and lattice instability in tungsten-rhenium alloys, *J. Nucl. Mater.* 278 (2000) 273–276.
- [73] Z. Liu, Y.A. Chang, Evaluation of the thermodynamic properties of the Re-Ta and Re-W systems, *J. Alloys Compd.* 299 (2000) 153–162.
- [74] X.S. Kong, Y.W. You, X.Y. Li, X. Wu, C.S. Liu, J.L. Chen, G.N. Luo, Towards understanding the differences in irradiation effects of He, Ne and Ar plasma by investigating the physical origin of their clustering in tungsten, *Nucl. Fusion* 56 (2016) 106002.
- [75] M.J. Baldwin, R.P. Doerner, Helium induced nanoscopic morphology on tungsten under fusion relevant plasma conditions, *Nucl. Fusion* 48 (2008) 035001.
- [76] D. Dasgupta, R.D. Kolasinski, R.W. Friddle, L. Du, D. Maroudas, B.D. Wirth, On the origin of ‘fuzz’ formation in plasma-facing materials, *Nucl. Fusion* 59 (2019) 086057.
- [77] K.B. Woller, D.G. Whyte, G.M. Wright, Impact of helium ion energy modulation on tungsten surface morphology and nano-tendrils growth, *Nucl. Fusion* 57 (2017) 066005.
- [78] R.P. Doerner, D. Nishijima, S.I. Krashennnikov, T. Schwarz-Selinger, M. Zach, Motion of W and He atoms during formation of W fuzz, *Nucl. Fusion* 58 (2018) 066005.
- [79] S. Kajita, N. Yoshida, R. Yoshihara, N. Ohno, M. Yamagiwa, TEM observation of the growth process of helium nanobubbles on tungsten: nanostructure formation mechanism, *J. Nucl. Mater.* 418 (2011) 152–158.
- [80] P. Filips, N. Connolly, D.N. Ruzic, Experimental mechanistic investigation of the nanostructuring of tungsten with low energy helium plasmas, *J. Nucl. Mater.* 482 (2016) 201–209.
- [81] T. Koyanagi, N.A.P.K. Kumar, T. Hwang, L.M. Garrison, X. Hu, L.L. Snead, Y. Katoh, Microstructural evolution of pure tungsten neutron irradiated with a mixed energy spectrum, *J. Nucl. Mater.* 490 (2017) 66–74.